Some Examples of Risk Analysis in Environmental Problems - Keynote Talk *

David R. Brillinger, University of California, Berkeley

December 10, 2002

Abstract

Risk analysis, that is the problem of estimating the probabilities of rare and damaging events, unifies the geosciences. One can mention the risks from: floods, earthquakes, forest fires, space debris. The probabilities may be fed into the computaion of insurance premiums. The Poisson process often plays a prominent role, while marked point processes have a basic function. Various ways to collect and extrapolate data will be described and examples from various fields will be presented. The topic unifies the environmental sciences.

1 Introduction.

1.1 Risk.

Risk may be defined as the probability of some hazardous event or catastrophe, the chance something bad will happen. In many cases huge amounts of money are involved [24]. The principal concern is low probability - high consequence events, events that lead to damage, loss, injury, death, environmental impairment for example. Often the work is done as an aid to decision making. In consequence risk models and risk management pervade modern technical life.

A common tool in the work is a *catastrophe model*. These have been defined as: a set of databases and computer programs designed to analyze the impact of different secenarios on hazard-prone areas [24]. In practice these models combine scientific risk assessments of the hazard with historical records to estimate the probabilties of disasters of different magnitudes and the resulting damage to affected structures. The information may be presented in the form of expected annual losses and/or the probability that in a given year the claims will exceed a certain amount.

Risk analyses may be required by the government. The end result may be a rate rather than a probability. To cite a specific example a Core Damage Frequency (CDF) value of 10^{-4} per reactor year is the value endorsed by the

*Supported by NSF Grants DMS 97-04739, DMS 99-71309 and DMS 02-03921.

Nuclear Regulatory Commission in a Staff Requirements Memorandum as a benchmark objective for accident prevention [26]. This rate is the probability of damage to a reactor core within a year. Its units may be viewed as number of events per year. See [11].

The field of risk analysis cuts across the environmental sciences. Here we focus on some geophysical risks, risks of things like: landslides, avalanches, earthquakes, floods, huricanes, tornadoes, forest fires, space debris, sea storms, and hail storms, ...

A formal risk analysis often includes: i) estimation of probabilities, ii) determination of the statistical distribution of damage and iii) preparation of products like formulas, graphics, hazard risk maps. There is extensive use of computing science, substantive subject matter and statistical methods.

A pair of revealing examples are provided by the papers of Fairley, [12], and Miller and Leslie, [21]. The Fairley work is concerned with the probability of a spill of liquified natural gas during its importation at U.S. ports. In particular the paper makes the case for describing risks by probabilities not by their reciprocals i.e. return periods, (the mean interval between events). The Miller-Leslie paper concerns the probability of a ship hitting the Tasman Bridge at Hobart, Austalia. In both these papers there is careful evaluation of the probabilities of component events.

1.2 Some basic concepts.

The tools of risk analysis include: statistical methods, substantive background, computer software and hardware. The products include probability estimates, hazard maps, decisions.

Among the pertinent statistical concepts are: borrowing strength, forecasting, (marked) point processes, Bayes Theorem, influence diagrams, uncertainty estimation, distributions, models (extreme value, threshold, Poisson, binary response, nonparametric and nonparametric methods).

Ideas from systems analysis and computing science also prove extremely useful in risk analyses. These include: box and arrow diagrams, software packages, simulation, decision tools, GIS, visualization, and data base management.

Both statistics and computer science often adopt the strategy of breaking the problem down conceptually.

2 Some examples of risk analyses.

2.1 Example 1 - Amazon Floods.

The first example concerns the risk of floods on the Amazon River. A renewal model is employed for the times of events, in part because the data set is small.

Manaus is a city well up the Amazon in Central Brazil. At a dock the river's height has been recorded daily since 1903. Also there are newspaper records and journals that may be consulted to determine the dates of some earlier floods. [31]. Of official concern is the question of whether the risk of flooding is increasing. Increased flooding will eventually occur because of the deforestration taking place ibid.

The top panel of Figure 1 provides the dates of floods. There were 21 of them during the period 1892 to 1992. The definition take for a flood, when specific measurements were available, was that the stage exceeded 28.5m. In the panel the dates are indicated by points along the x-axis and points of increase in the cumulative count function $N(t)$. To estimate the hazard function one needs a distribution function for the times between events. The histogram of the times between successive floods is given in the middle panel of Figure 1. The long tail suggests the use of a Pareto distribution with p.m.f. $p(u) = C_\alpha/u^\alpha,\ u = 1, 2, 3, \ldots$. The domain is integers because the data employed are years. The curve fit by maximum likelihood is superimposed in the second panel. It is assumed that the times bewteen events are independent, i.e. the point process is renewal.

The bottom panel provides an estimate of the hazard as a function of time since the last year of the data employed in our analysis, 1992. Approximate 90% confidence intervals are also indicated. These were obtained by working with the logit transform and employing the delta-method.

More details of the analysis may be foiund in the papers [31], [3].

2.2 Example 2 -Great Earthquakes in California.

The concern of this example is probabilities for future great earthquakes in Southern California. Once again a renewal process is employed, i.e. the times between events are assumed i.i.d..

Pallett Creek is a location northeast of Los Angeles that is astride the San Andreas Fault.. It has interesting geological structure. In the early eighties the paleogeologist Kerry Sieh dug a trench that crossed the San Andreas Fault there [29]. The trench showed an interesting structure - a number of sedimentary layers were visible. There were breaks in the layers and Sieh inferred that these were due to great earthquakes. For most of the breaks he was able to collect samples of material that could be dated by radiocarbon (RC) methods. Sieh carried out further studies. The estimated dates of earthquakes whose presence he inferred are shown in Figure 2.

The analysis here is interesting for: the small number of data points involved, the presence of a missing value, an open interval and substantial measurement error. In order to obtain estimates of risk a renewal process with a Weibull distribution is hypothesized for the intervals between the events. The Weibull

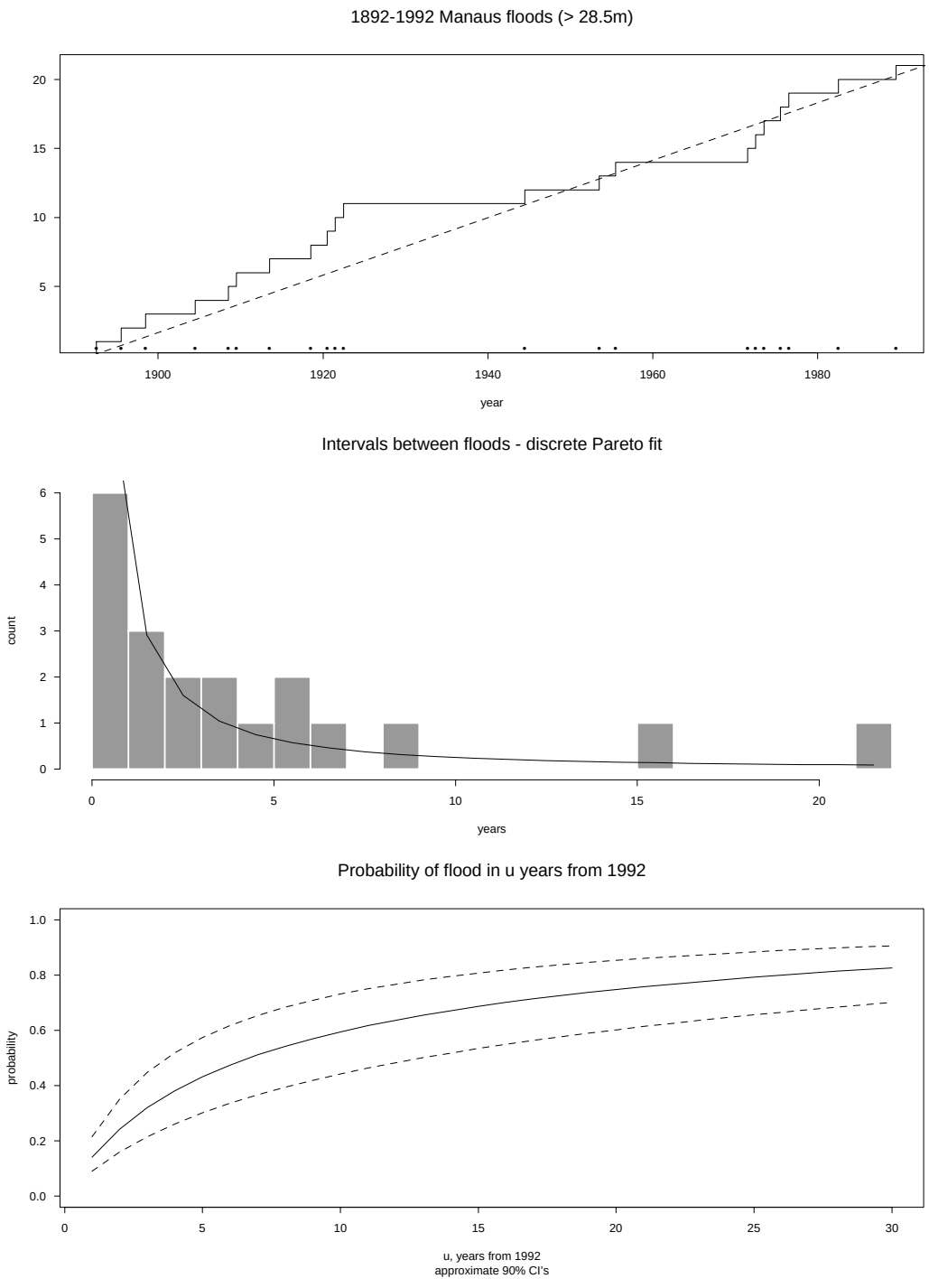

Figure 1: Panel 1 is a step function counting the number of floods since January 1892. The dashed line's slope provides the rate of events. Panel 2 is the histogram of the intervals between floods and a fitted Pareto. Panel 3 is the estimate of the hazard function and approximate 90% confidence intervals.

density is

$$Prob\{interval \leq x\} = 1 - exp\{-(x/\alpha)^{\beta-1}\},\ x > 0$$

Measurement error from the radiocarbon dating is modelled as additive normal with mean 0 and s.d. estimated at the RC laboratory. The missing date for an event meant taking one of the available intervals as the sum of two Weibulls. The open interval starts at the last event. It occurred in 1857. Numerical integration was employed to determine the density of a Weibull plus an independent normal and the one for the sum of two Weibulls. The reasonableness of the Weibull assumption was assessed by the Weibull hazard plot given as the middle panel of Figure 2. Maximum likelihood analysis was employed to estimate the parameters. More details may be found in [30].

The bottom panel of Figure 2 gives the estimated risk as a function of years into the future from 1988. The figure also includes approximate 95% marginal confidence bounds.

2.3 Example 3 - Earthquake Damage.

Cornell [10] is the seminal paper on seismic risk assessment (SRA). His definition of the subject is a variant of the following:
Seismic risk assessment - the process of estimating the probability that certain performance variates at a site of interest exceed relevant critical levels within a specified time period as a result of nearby seismic events.

The approach presented here is one of breaking the problem down conceptually into manageable parts: a) damage, b) site, c) attenuation and d) event locations, times and sizes. These parts are illustrated in Figure 3.

In computing risks generally and seismic risks particularly two probability results are basic:
Bayes Rule

$$P(ABC...) = P(A)P(B|A)P(C|AB)... \tag{1}$$

Total probability theorem

$$P(A) = \sum_k P(A|B_k)P(B_k) \tag{2}$$

[34] is another fundamental paper. Figure 3 shows the corresponding series and parallel structure for two possible events.

In the presentation we work backwards from a structure at a site to the locations, times and sizes of earthquakes. (Two events are illustrated in the Figure.)
a) *Damage.* There are a variety of ways to describe and estimate damage. An important method uses the Modified Mercalli Intensity (MMI). One reason for its importance is that values may be derived from historic accounts. Another is that it refers to damage directly.

MMI values are given by roman numerals I to XII (and sometimes 0 referring to no impact.) The scale is ordinal increasing with increasing severity of damage.

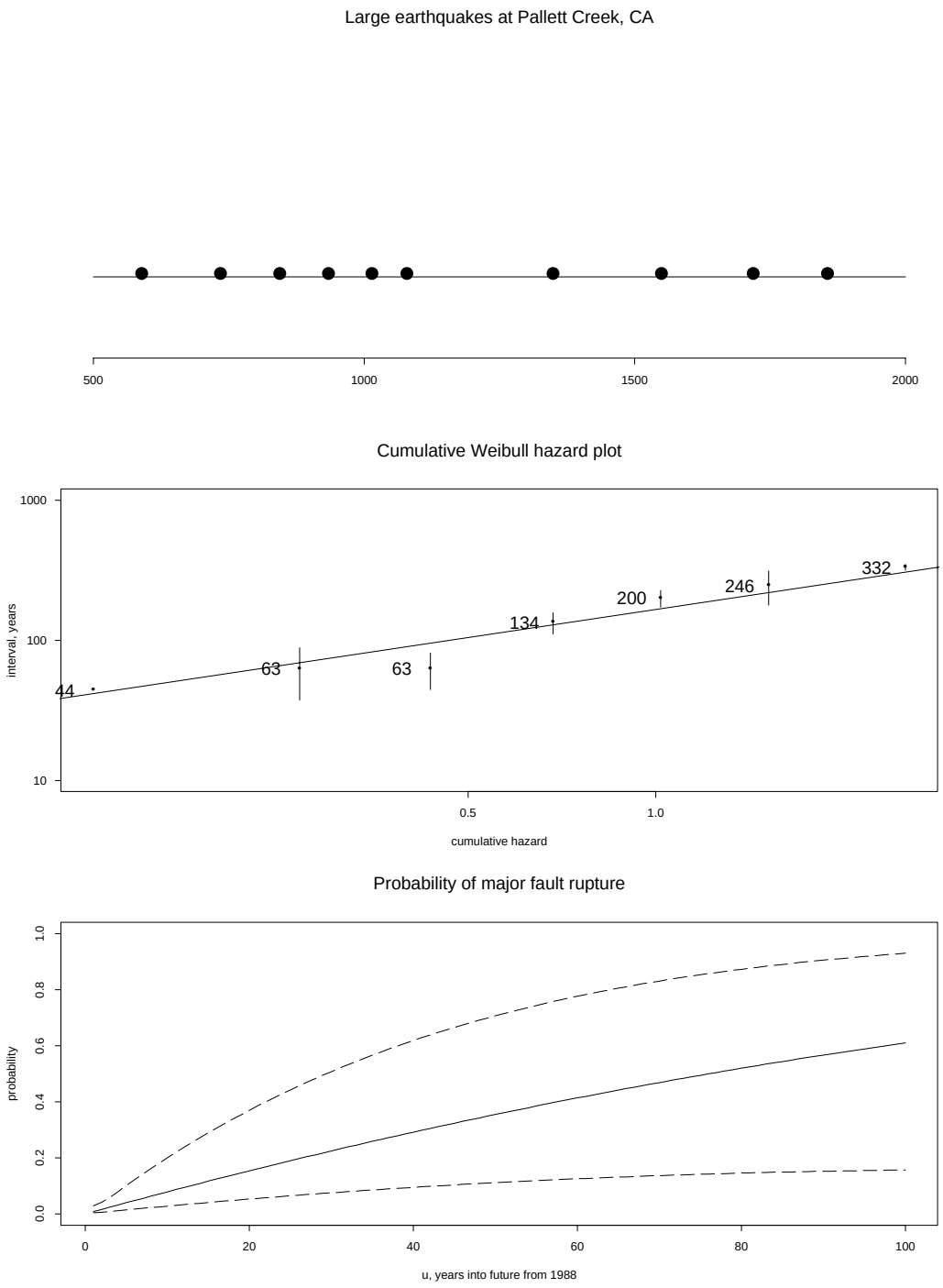

Figure 2: Panel 1 estimated dates of the Pallett Creek events; panel 2 Weibull hazard plot with the vertical lines indicating twice the RC dating s.e.'s; bottom panel the estimated risk.

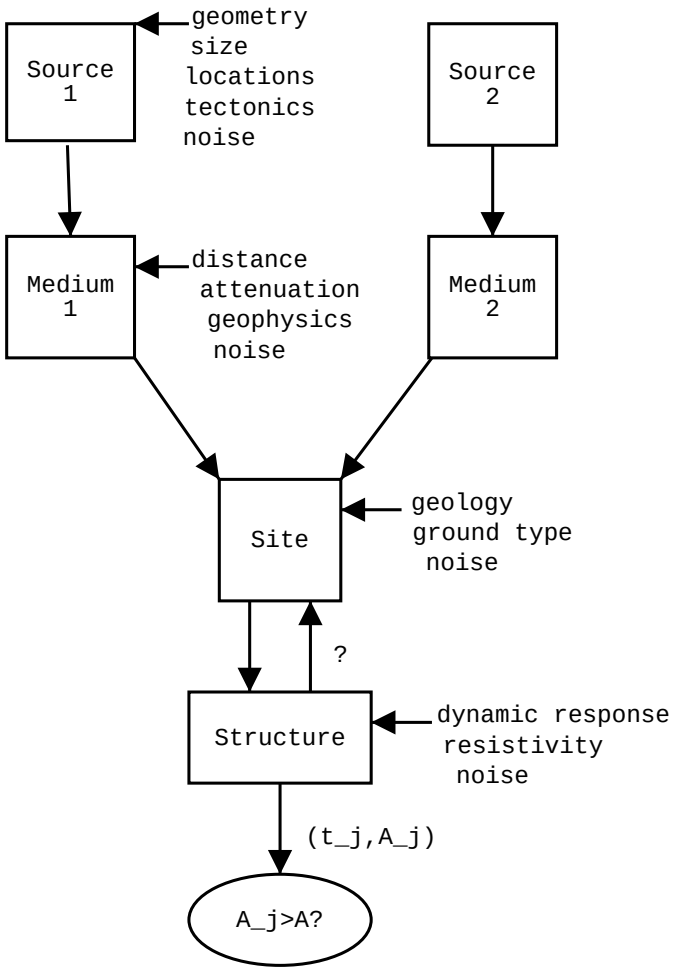

Figure 3: Box and arrow diagram highlighting components of an SRA. A_j refers to the level of some performance variate occurring with the j-th event. A is a threshold level at which damage occurs.

For example the definition of MMI VIII includes: "Damage slight in specially designed structures; considerable in ordinary substantial buildings; ..." [7].

There are values that have been proposed to convert MMI values into damage percentages for different types of structures. The following is an example of a so-called damageability matrix given in [23]. The entries are loss ratios per risk category in %.

MMI	VI	VII	VIII	IX	X
residential	.4	1.7	6	17	42
commercial	.8	3	11	27	60
industrial	.1	.7	3	11	30

Figure 4 shows some of the MMI-values obtained following the Loma Prieta event of 17 October 1989. Th two large bays are San Francisco Bay and Monterey Bay. Only some of the observations are plotted to avoid overstriking. The epicenter of the event was near Santa Cruz California. (Arabic numerals are plotted rather that Roman for convenience.) See also [32].

Next we seek a spatial distribution for the MMI values. Ordinal data are conveniently handled by postulating the existence of a latent variable ζ and cut points a_i such that the MMI value at location (x, y) is given by

$$I_{x,y} \;=\; i \; if \; a_i \;<\; \zeta_{x,y} \;\leq a_{i+1}$$

Continuing we postulate a model

$$\zeta_{x,y} \;=\; f_{x,y} \;+\; \epsilon_{x,y}$$

with $f_{x,y}$ deterministic and smooth and with $\epsilon_{x,y}$ having an extreme value distribution. The use of the extreme value distribution is plausible given the nature of destruction. It and the corresponding cloglog link mean that the function glm() may be used for the computations, see McCullagh and Nelder [20], Chapter 5.

In [5] $f_{x,y}$ is estimated using the generalized additive models fitter gam() of Hastie and the smoother loess() of Cleveland [9], on data from the Loma Prieta event employed. Figure 5 provides the estimate of f. One see a general dying off of the function values as one moves away from the epicenter, except for a rise near San Francisco. This increase is associated with reclaimed land.

b) *Attenuation.* Next a relationship describing the fall-off in energy with distance as it passes through the medium is needed. This general fall-off is apparent in Figure 4. Following Joyner and Boore, [17], consider the attenuation form

$$(3) \qquad log(-log(1 \;-\; Prob\{I = i\})) \;=\; \alpha_i \;+\; \beta d \;+\; \gamma log(d) \;+\; \delta M$$

where d is the distance of the observation point to the epicenter of the event and M the event's magnitude. This was fit to the Loma Prieta data. (As only one event was involved δ could not be estimated separately of the α_i.). The results are given in Figure 6. In the case of MMI VIII one sees a very rapid fall-off with distance.

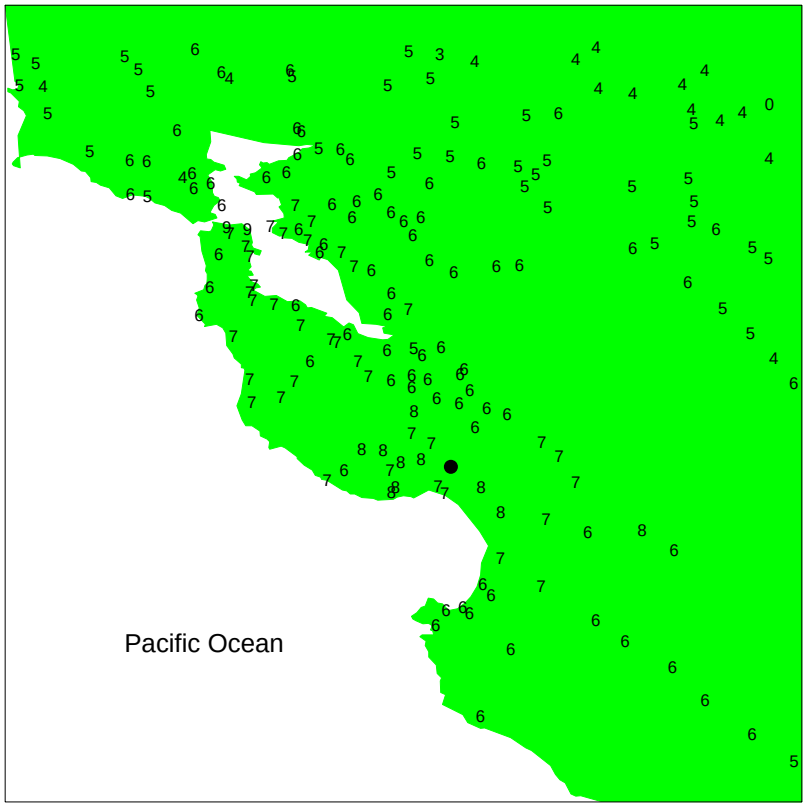

Figure 4: A sampling of MMI values observed for the Loma Prieta Earthquake. The circlar dot represents the epicenter of the event.

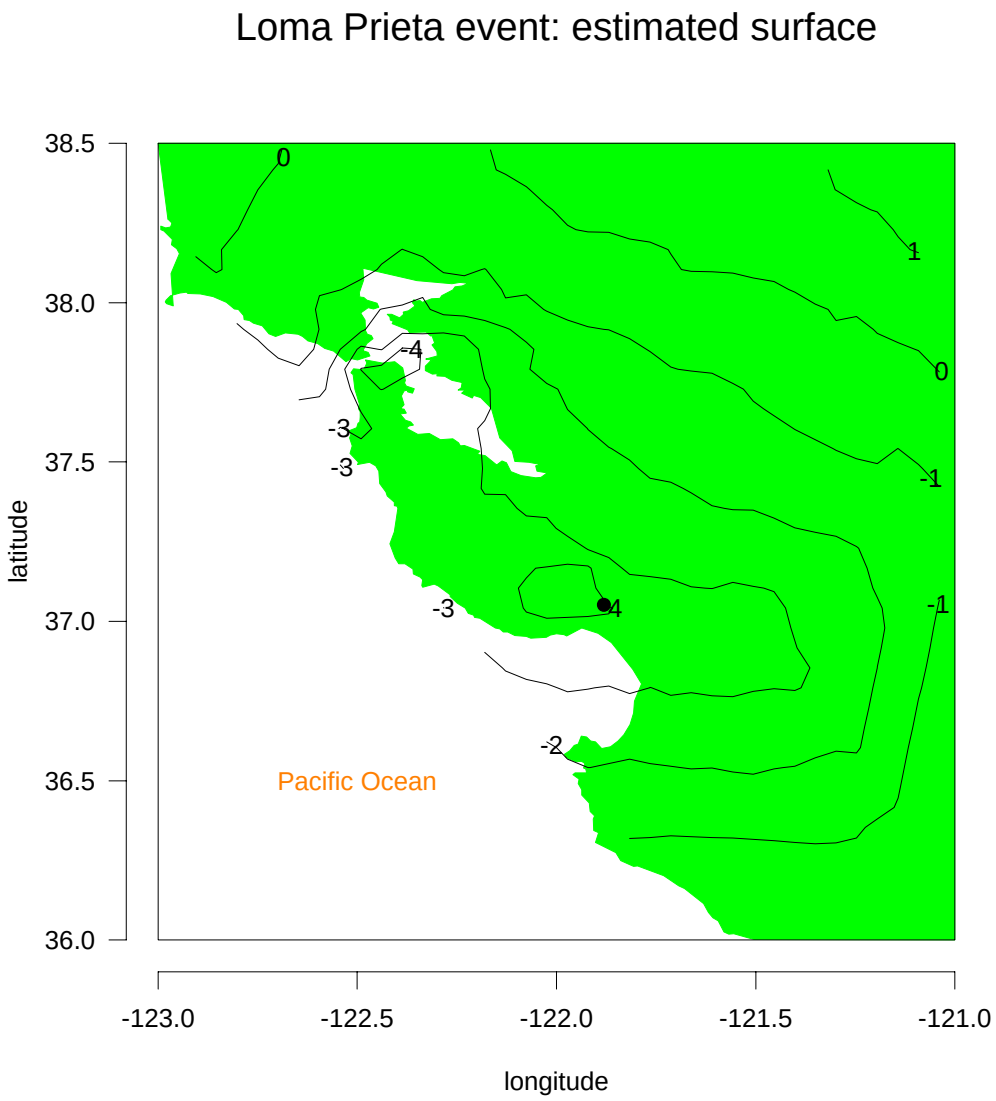

Figure 5: The estimate of the surface $f_{x,y}$.

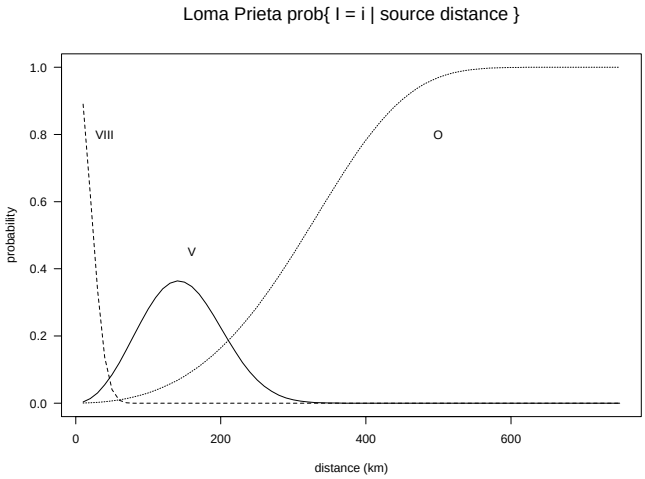

Figure 6: Fitted probabilities of the indicated MMIs as a function of distance from the epicenter.

c) *Event locations and times.* One imagines a marked spatial-temporal point process of earthquake locations, times and sizes, (x_i, y_i, t_i, M_i). In California many faults have been located. In Figure 3 just two sources have been hypothesized, but there could be many. One uses the total probability theorem (2). In an expression like (3) one might take d to be the distance to the nearest point on the fault from the site. Faults have been modelled as line and plane segments with event magnitude related to their size. There are many geological fault maps to work with.

Commonly renewal processes are employed to model the sequence of times. The intervals between events might be assumed exponential, Weibull or lognormal.

As an example of a fair premium computation, consider a commercial building 25km from an epicenter and an event like Loma Prieta. For this case the estimated expected loss is

$$.8 * .102 + 3 * .389 + 11 * .475 \;=\; 6.47\%$$

and so the fair premium would be 6.47% of the amount insured.

See [2] for further details concerning this example.

2.4 Example 4 - Forest Fires.

In this example we turn to the problem of predicting the occurrence of forest fires as a function of place and time. Let occurrences be denoted by (x_j, y_j, t_j), $j = 1, 2, 3, \ldots$. One has a point process in space and time.

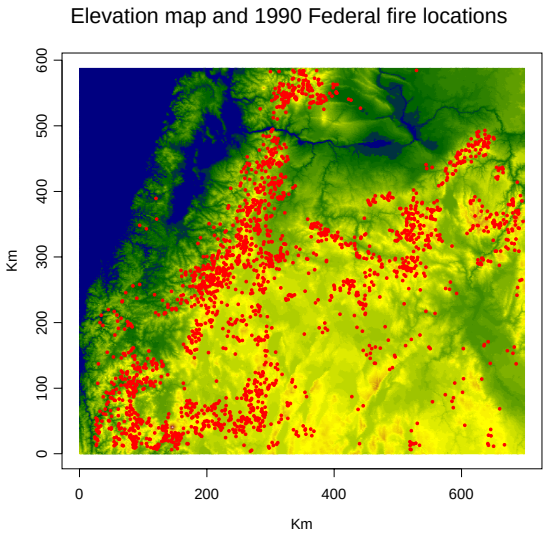

Figure 7: Locations of fires in Oregon during 1989-1996

To illustrate the idea consider Figures 7 and 8. Figure 7 shows the locations of forest fires in Oregon during the period 1989-1996 that occurred in Federal lands. These lands are indicated in Figure 8.

Consider voxels $(x, x+dx] \times (y, y+dy] \times (t, t+dt]$ and let

$$N_{x,y,t} \;=\; 1 \qquad if\ a\ fire\ in\ the\ (x,y,t)\ voxel$$

$$=\; 0 \qquad otherwise$$

For convenience suppose that $dx,\ dy,\ dt \;=\; 1$. (In the data and computations $dx,\ dy \;=\; 1km$ and dt is 1 day. Letting H_t denote the history of the process up to time t, consider the probability

$$Prob\{N_{x,y,t} \;=\; 1 \mid H_t\} \;=\; p_{x,y,t}$$

In the work a logit model was assumed, specifically

$$logit\ p_{x,y,t} \;=\; g_1(x,y) \;+\; g_2(d) \;+\; \zeta$$

with (x, y) - location, d - day of the year, ζ year effect. The g functions are assumed to be smooth in the computations and are represented by spline functions. The spatial term, g_1, involved a thin plate spline and the day term, g_2, was a spline with period one year. The function took the form

$$g_1(x,y) \;=\; \alpha \;+\; \beta x \;+\; \gamma y \;+\; \sum_{j=1}^{J} \delta_j r_j^2 log\ r_j$$

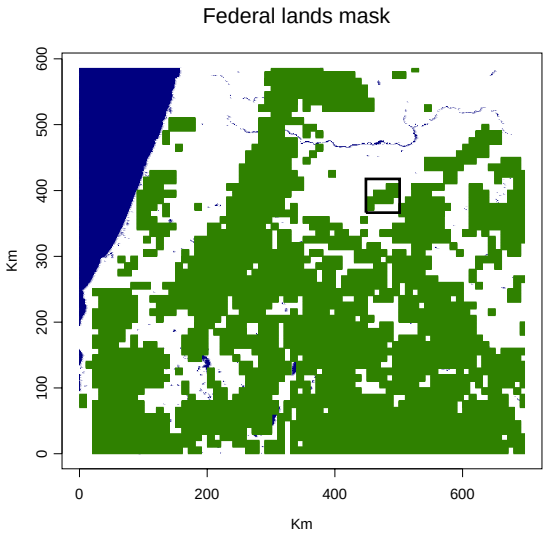

Figure 8: Federal lands in Oregon

where for nodes (x_j, y_j) the distance is $r_j^2 = (x - x_j)^2 + (y - y_j)^2$, [27]. The Splus function make.rb() of Funfits, [13], was employed in the computations. Logit models have been used previously in estimating fire risk, see for example [19].

The data set for Oregon was very large, 578,192,400 voxels and 15,786 fires. To be able to carry out exploratory data analyses a sample of the data used. All the voxels with fires were employed, but only a sample of those where no fires occurred. The sampling fraction was $\pi = .00012$ This lead to 58094 cases for the analysis.

With the logit link, conditional on the sample one had a generalized linear model (glm) with an offset of $log\ 1/\pi$. This meant that standard glm computer programs could be used for the analysis. (The new logit was $logit\ p' = logit\ p + log(1/\pi)$.)

The results are provided in Figure 9. One has estimates of the functions g_1, g_2 and the effects ζ. The ζ are assumed fixed, but in work in progress they are random. Examining the top panels one sees fewer fires in SE Oregon, as could have been anticipated from Figure 7. In the thin-plate computations 60 nodes were employed and they were taken to be 10km apart throughout the region. From the bottom left panel of Figure 9 one notes a definite day effect - more fires in the summer. From the bottom right panel there appears to be a definite year effect. The year effect values are relative to 1996 as 0. The horizontal line is at 0. Also in the bottom panels of the figure are ± 2 s.e. bounds.

One can get estimated probabilities for a nominated region and times by

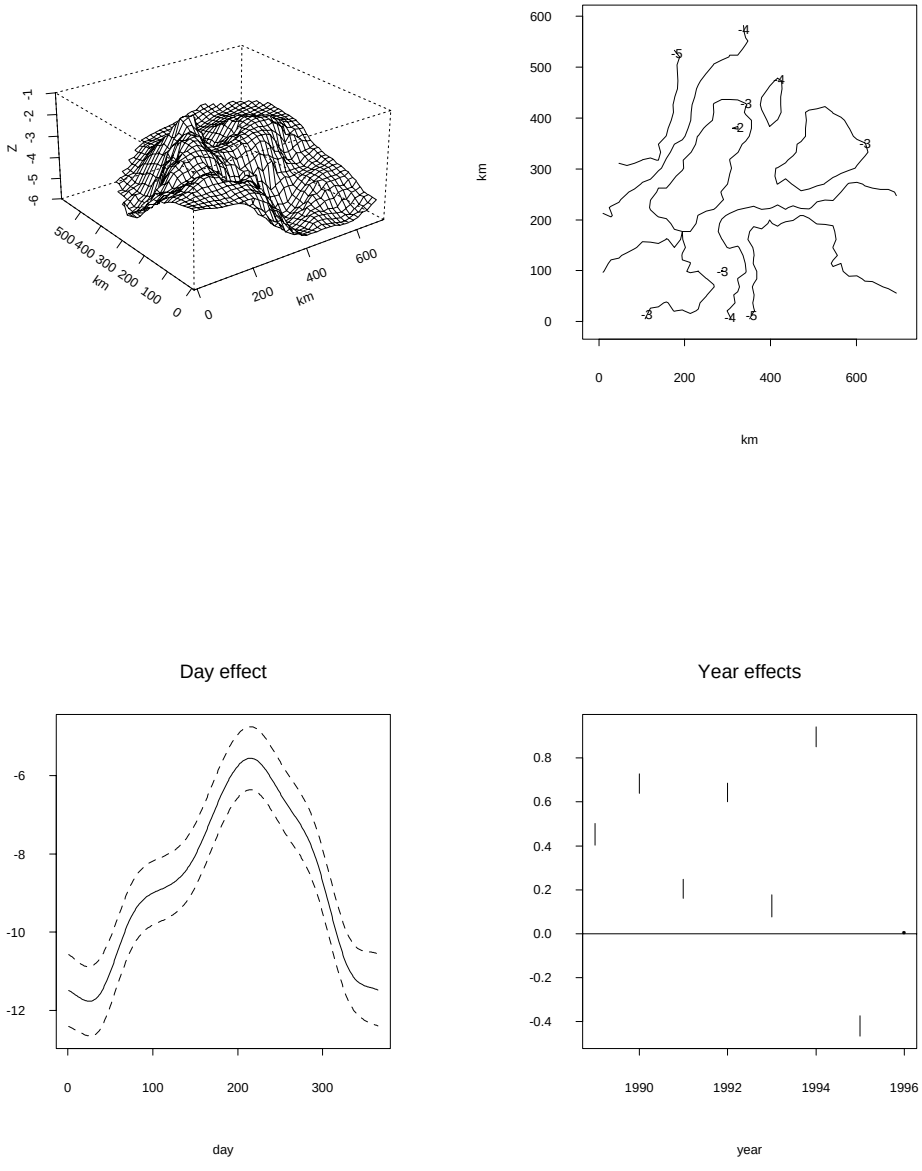

Figure 9: Top panels - estimated location effect, $\hat{g}_1$ in perspective and coutour form. Bottom left panel - estimated day effect. Bottom right panel - estimated year effects. Approximate 95% error bounds are indicated.

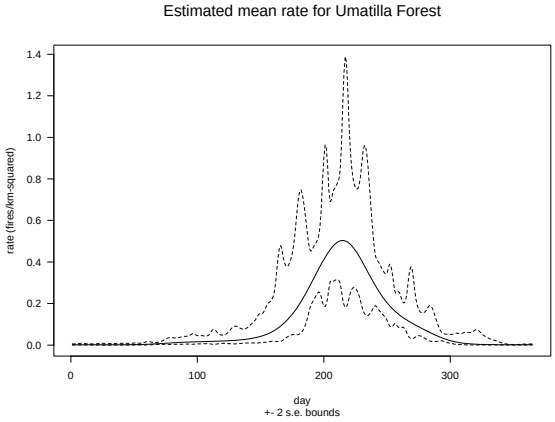

Figure 10: Estimated rate of fires (fires/km-squared/day) for the Umatilla Forest region.

adding voxel values. This is done for the Umatilla Forest and the results are presented in Figure 10. (This region is the green area within the rectangle of Figure 8. Also in the bottom panels of the figure are ± 2 s.e. bounds.). The count of fires in the region will be approximately Poisson following the Hodges-Le Cam result [14]. This may be used to obtain estimated probabilities of, for example, the number of fires in a specified time period exceeding a specified count.

The above results are elaborated upon in [6], [28]. Currently the work is involving other explanatories, random year effects and extensions to other states of the U.S. . An example of a meteorological variable is moisture level, see Figure 11.

2.5 Example 5 - Space Debris.

The space near the Earth has been described as a veritable garbage can. There are now in orbit millions of pieces of debris. These result from space activities over the last 45 years. More than 200,000 of the pieces are between 1 and 10cm in size. They orbit at speeds of several kilometers per second and can cause substantial damage if they hit another object. In designing shielding for a space object it is important to know the risks of collisions, [25], [15], [1].

An example of a question that arises is: What is the chance of some 1-10 cm piece of debris passing through the $11000m^2$ cross-section of the International Space Station space in the next 15 years? We will consider a simple variant.

There is considerable scientific knowledge of the physics of orbits dating back to Kepler and Newton, see [33]. It may be used to estimate risks, [16], [8], [18].

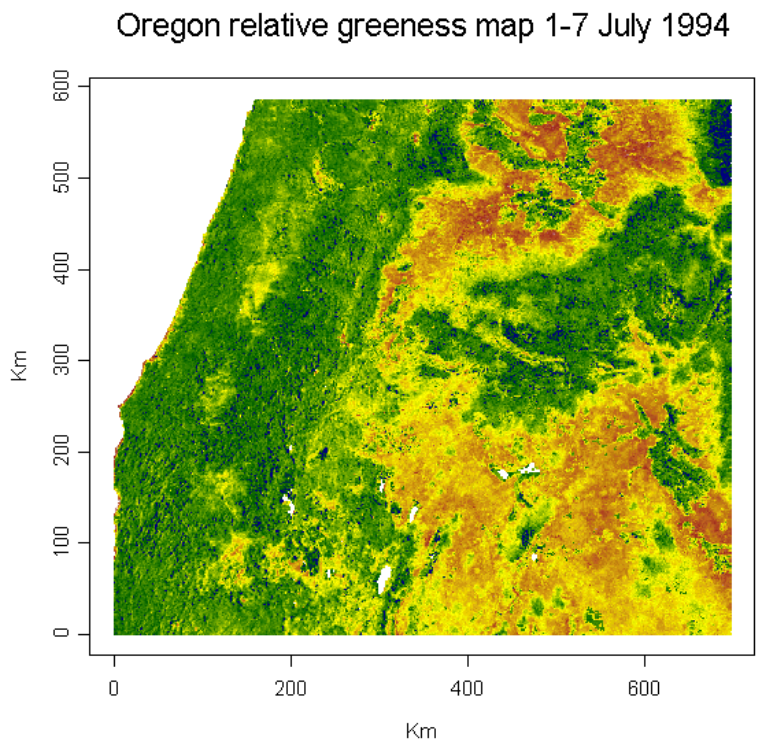

Figure 11: Moisture level for a week in July 1994

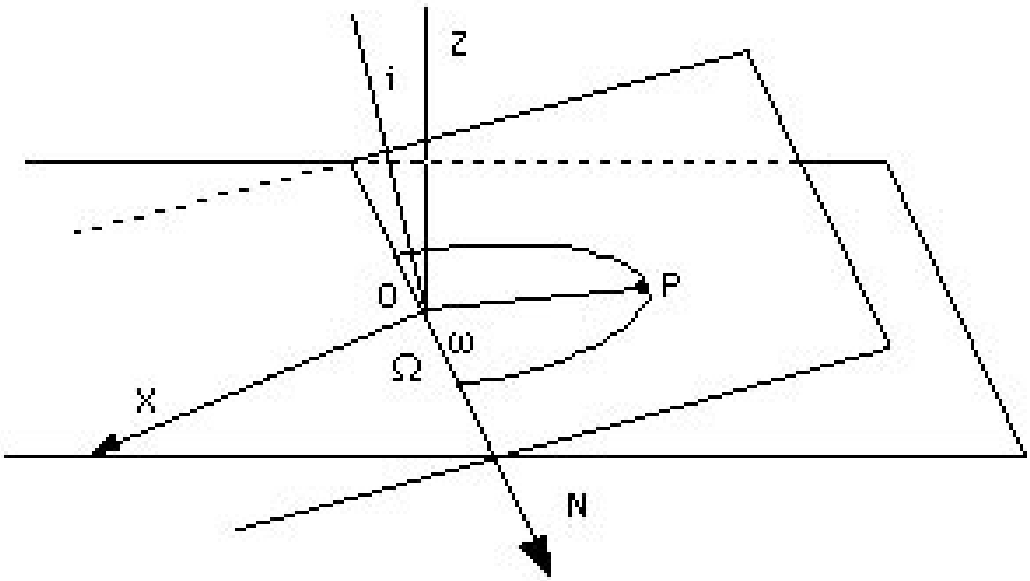

Figure 12: A three dimensional representation of the orbit of an object showing the elliptical orbit in the plane of rotation.

Figure 12 is taken from the NASA site www-istp.gsfc.nasa.gov/stargaze/Smotion.htm . It shows the character of orbits and sets up some notation. In the figure: X is the direction to the Vernal Equinox, N is the direction of the Ascending Node, Ω is the Right Ascension, P is the point of Perigree, i is the inclination, ω is the argument of Perigee . A basic aspect of the motion of an orbiting object is that it takes place in a plane and is elliptical, [33] and [22]. This is illustrated in the Figure.

For the moment considerations and notation are restricted to the case of the plane. Figure 13 shows a quarter of an orbit. The Earth is at the focus, O, and at time t the object is at P which will be described by (f_t, r_t) using polar coordinates with f_t, the *true anomaly*. A related angle is E_t, the *eccentric anomaly*. These variables are illustrated in Figure 13. The elliptical orbit may be represented as

$$r_t \ = \ a(1 - e \ cos \ E_t)$$

where a is the semimajor axis and e the eccentricity of the ellipse. The ellipse is swept out as E_t varies. In terms of Figure 13 the object is at (ϕ_t, r_t) where $\phi_t \ = \ \omega + f_t$.

The equations of motion may now be written

$$cos \ f_t \ = \ (cos \ E_t \ - \ e)/(1 \ - \ e \ cos \ E_t),$$

$$sin \ f_t \ = \ \sqrt{1 - e^2} sin \ E_t \ /(1 \ - \ e \ cos \ E_t)$$

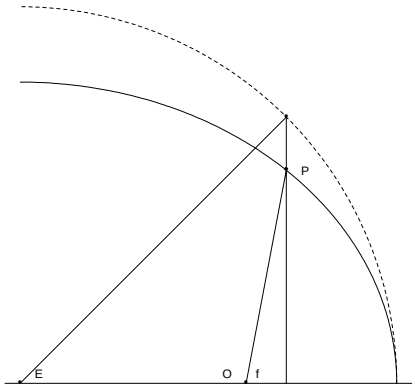

Figure 13: The solid line represents a quarter of an orbit. The point O, the focus of the ellipse, represents the Earth. The point P is the position of the object on its orbit. The angle f is the true anomaly. The angle E is the eccentric anomaly. The dashed line is the circumscribing circle.

$$n(t-T) \;=\; E_t \;-\; e\ sin\ E_t$$

The last is $Kepler's Equation$. The constant n is the *mean motion* and $P \;=\; 2\pi/n$ is the period.

The paper [4] considers the rate of objects passing through a patch of space and develops results using traditional statistical methods. Previous researchers had used ergodic arguments in most part. In this 2-dimensional case a patch is defined, in polar coordinates, by

$$\{(\phi = a(u), r = b(u)),\ u\ \epsilon\ U\} \tag{4}$$

It is shown in [4] that the expected rate of objects passing through the patch is

$$\int_E \int_U p\left(a(u) - atan(\sqrt{1-e^2}sinE, cosE \;-\; e), t - \frac{1}{n}(E \;-\; esinE)\right)\delta\left(a(1 \;-\; cosE) \;-\; b(u)\right)$$

$$\cdot|a'(u)aesinE \;-\; b'(u)\frac{\sqrt{1-e^2}}{1 \;-\; ecosE}|\ du\ dE \tag{5}$$

where $p(\omega, T)$ represents the joint density of ω and T and δ is the Dirac delta function.

Consider the particular case of a line segment poining directly at O. It may be represented by $\phi \;=\; \phi_0,\ r \;=\; r_0 + u$ with $0 \;<\; u \;<\; \epsilon$. Suppose that ω is uniform on $(0, 2\pi)$ and independently T is on uniform $(0, P)$, i.e. the initial conditions are random. The rate function is then

$$\frac{a\sqrt{1-e^2}}{r_0}\frac{1}{\sqrt{(r_0-q)(q'-r_0)}}\frac{\epsilon}{\pi P} \tag{6}$$

where $q,\ q' \;=\; a(1-e),\ a(1+e),\ q < r < q',\ 0 \leq \phi < 2\pi$. This quantity does not depend on t, nor does it depend on ϕ_0, as could have been anticipated. The function is graphed in Figure 14 for the case of eccentricity .6 . The function depends strongly on r. One sees higher rates at the extremes, $q,\ q'$, of the orbit with the highest at q.

In reality there are many orbiting objects. Their effects are superposed. They, i.e. their initial conditions, may be independent or they may be dependent as they result from the same breakup.

There are also important explanatories, such as solar pressure, drag, to include in a model.

3 Discussion and Conclusions.

The demand for risk analyses is growing generally, in part because costs of replacing destroyed structures are growing and in part because of the steady increase in the population living in hazardous areas. Statistical methods are basic to risk assessments. This is obvious because probabilities and data are

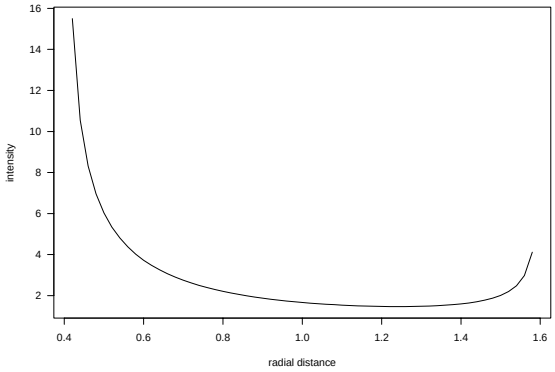

Figure 14: The rate function (6).

involved. It is also the case because statistics adds important things to what the engineers and scientists tend to know and do on their own. Statisticians add things like efficiency results, extensions to different data types, and uncertainty analyses.

What have we learned from the examples presented? There are difficulties and opportunities. There are solutions and there are lots of open problems. The stochastic approach is highly effective.

What do the 5 examples have in common? - They are seeking probabilities and distributions. What do the solutions have in common? - Data and subject matter are basic. What are the products for each example? - Estimated probabilities. Which methods play an important roles? - Stochastic modelling and CI construction.

Acknowledgments.

Collaborators are basic to work on problems of the type considered. Mine include: Floods - Hilgard O'R. Sternberg, Great earthquakes - Kerry Sieh; MMI - Chiann Chang, Pedro Morettin, Rafael Irizarry; Fires - John Benoit, Haiganoush Preisler; Space debris - Abdel El-Sharaawi and the researchers at Johnson Space Center.

People who provided help concerning the computing includied Doug Bates, Chong Gu, Trevor Hastie and Phil Spector.

Part of the material was peresented in the keynote talk presented at the 2002 Interface Meeting in Montreal. I thank Ed Wegman for the invitation.

References

[1] BARTON, D. K., BRILLINGER, D. R., EL-SHAARAWI, A. H., MCDANIEL, P., POLLOCK, K. H. and TULEY, M. T. (1998). *Final Report of the Haystack Orbital Debris Data Review Panel*. Johnson Space Center, Tech. Mem. 4809.

[2] BRILLINGER, D. R.(1993). Earthquake risk and insurance. *Environmetrics* 4, 1-21.

[3] BRILLINGER, D. R. (1994). Trend analysis: time series and point process problems. *Environmetrics* 5, 1-19.

[4] BRILLINGER, D. R. (2001). Space debris: flux in a two dimensional orbit. Pp. 105-116 in *Statistics and Genetics in the Environmental Sciences*. (Eds. L. T. Fernholz, S. Morgenthaler and W. Stahel). Berkhauser Verlag, Basel.

[5] BRILLINGER, D.R., CHIANN, C., IRIZZARY, R.A. and MORETTIN, P.A. (2001). Automatic methods for generating seismic intensity maps. *Probability, Statistics and Seismology: Journal of Applied Probability* Vol. 38A, 189-202.

[6] BRILLINGER, D. R., PREISLER, H. K. and BENOIT, J. W. (2003). Risk assessment: a forest fire example. In press.

[7] BULLEN, K. E. and BOLT, B. A. (1985). *An Introduction to the Theory of Seismology, Fourth Edition*. Cambridge, Cambridge.

[8] CLEGHORN, G. E. A. (1995). *Orbital Debris: a Technical Assessment*. National Academy Press, Washington.

[9] CLEVELAND, W. S., GROSSE, E. and SHYU, W. M. (1992). Local regression models. Pp. 309-376 in *Statistical Models in S*. (Eds. Chambers, J.M. and Hastie, T.J.). Wadsworth, Pacific Grove.

[10] CORNELL, C. A. (1968). Engineering seismic risk analysis. *Bull. Seismol. Soc. Amer.* 58, 1583-1606.

[11] ELLINGWOOD, B. (1994), *Validation of Seismic Probabilistic Risk Assessment of Nuclear Power Plants*. U. S. Nuclear Regulatory Commission, GPO Washington.

[12] FAIRLEY, W. B. (1977). Evaluating the "small" probability of a catastrophic accident from the marine transportation of liquefied natural gas. Pp. 331-354 in *Statistics and Public Policy* (Eds. W. B. Fairley and F. Mosteller). Addison-Wesley, Reading.

[13] FUNFITS (2002). www.cgd.ucar.edu/stats/Software/Funfits

[14] HODGES, J. L. and LE CAM, L. M. (1960). The Poisson approximation to the Poisson Binomial distribution. *Ann. Math. Statist.* 37, 737-740.

[15] JOHNSON, N. L. (1998). Monitoring and controlling debris in space. *Scientific American* 62-67.

[16] JOHNSON, N. L. and MCKNIGHT, D. S. (1987). *Artificial Space Debris*. Orbit Book Co., Malabar.

[17] JOYNER, W. B. and BOORE, D. M. (1981). Peak horizontal acceleration and velocity from strong-motion records including records from the 1979 Imperial Valley, California, earthquake. *Bull. Seism. Soc. Amer.*, 71, 2011-2038.

[18] KESSLER, D. J. (1981). Derivation of the collision probability between orbiting objects: the lifetimes of Jupiter's outer moons. *Icarus* 48, 39-48.

[19] MARTELL, D. L., Otukol, S. and Stocks, B. J. (1987). A logistic model for predicting daily people-caused forest fire occurrence. *Canadian J. Forest Research* 19, 1555-1563.

[20] MCCULLAGH, P. and NELDER, J. A. (1989). *Generalized Linear Models, Second Edition*. Chapman and Hall, London.

[21] MILLER, A. J. and LESLIE, J. S. (1979). The risk of collisions between ships and bridges. *Proc. 42nd Session of the ISI* 48, 137-148.

[22] MONTENBRUCK, O. and GILL, E. (2000). *Satellite Orbits*. Springer, Berlin.

[23] MUNICH RE (1991). *Insurance and Reinsurance of Earthquake Risk*. Munich Re, Munich.

[24] NATIONAL ACADEMY OF SCIENCE (1998). *Paying the Price*. (Eds. H. Kunreuther and R. J. Roth.) J. Henry Press, Washington.

[25] NATIONAL RESEARCH COUNCIL (1997). *Protecting the Space Station from Meteoroids and Orbital Debris*. NRC, Washington.

[26] NUCLEAR REGULATORY COMMISSION (1997). Federal Register: June 25, 1997, Volume 62, Number 122 Notices 34321-34326.

[27] POWELL, M. J. D. (1992). The theory of radial basis function approximation in 1990. *Advances in Numerical Analysis, Vol II*. (Ed. W. Light). Oxford, Oxford.

[28] PREISLER, H. K., BRILLINGER, D. R., BURGAN, R. E. and BENOIT, J. W. (2003). Probability based models for the estimation of wildfire risk. Submitted.

[29] SIEH, K. E. (1984). Lateral offsets and revised dates of large prehistoric earthquakes at Pallett Creek, Southern California. *J. Geophysical Res.* 89, 641-647.

[30] SIEH, K., STUIVER, M. and BRILLINGER, D. R. (1989). "A more precise chronology of earthquakes produced by the San Andreas Fault in Southern California," *J. Geophysical Research* 94, 603-623.

[31] STERNBERG, H. O'R. (1987). Aggrevation of floods in the Amazon River as a consequence of deforestration? *Geografiska Annaler* 69A, 201-219.

[32] STOVER, C.W., REAGOR, B.G., BALDWIN, F. and BREWER, L. (1990). *Preliminary Isoseismal Map For the Santa Cruz (Loma Prieta), California, Earthquake of October 18, 1989*. UTC: Open File Report 90-18. National Earthquake Information Center, Denver.

[33] SZEBEHLY, V. G. (1989). *Adventures in Celestial Mechanics*. University of Texas Press, Austin.

[34] VERE-JONES, D. (1973). The statistical estimation of earthquake risk. *New Zealand Statistician* 8, 7-16.